

Triazolyl Ru(II), Os(II), and Ir(III) Complexes as potential HIV-1 CCR5 inhibitors

Brandon Putterill[#], Charles Rono^{*}, Banothile Makhubela^{*}, Debra Meyer[†] –
Ntombenhle Gama^{#^}

[#] Department of Biochemistry, Genetics and Microbiology, Faculty of Natural and Agricultural Sciences, University of Pretoria, Pretoria, 0083

^{*} Research Center for Synthesis and Catalysis, Department of Chemical Sciences, Faculty of Science, University of Johannesburg, Johannesburg, 2006

[†] The Deans Office and Department of Biochemistry, Faculty of Science, University of Johannesburg, Johannesburg, 2006

[^] Corresponding author e-mail, ntombenhle.gama@up.ac.za

Abstract

Infection by the human immunodeficiency virus, which gives rise to acquired immunodeficiency syndrome, is still a major global health challenge, with millions of people being affected. The use of combination antiretroviral therapy has been a great success, leading to reduced mortality rates over the years. Although successful, these drugs are associated with various side effects, necessitating the development of new treatment strategies. This study investigated three metal-based complexes that were previously shown to possess some anticancer activity. The complexes were investigated against three pseudoviruses, which consisted of HIV-1 subtype C (CAP 210 and Du 156) and subtype A (Q 23). These complexes inhibited viral entry at low micromolar concentrations, with IC₅₀ values ranging from 5.34 to 7.41 μM for *N*-aryl-1H-1,2,3-triazole-based cyclometalated ruthenium-(II) (**A**), 2.35–8.09 μM for *N*-aryl-1H-1,2,3-triazole-based cyclometalated iridium-(III) (**B**) and 2.59–4.18 μM for *N*-aryl-1H-1,2,3-triazole-based cyclometalated osmium-(II) complex (**C**). This inhibition was significant, with no significant inhibition from the ligand alone at similar concentrations. Additionally, these concentrations were non-toxic to mammalian cells. The complexes were further analysed for their potential mechanism of action using *in silico* docking (Maestro 12.2), which indicated that the activity is potentially due to their interaction with the CCR5 co-receptor. The predicted interaction involved amino acids (Glu 283, Tyr 251 and Tyr 108) that are essential for the interaction of the chemokine receptor with viral gp120.

Keywords: HIV-1, Entry inhibition, Metallodrugs, Ruthenium complexes, Iridium complexes, Osmium complexes.

1 Introduction

It has been estimated by the WHO and UNAIDS that there are currently 38 million individuals living with HIV globally, with an estimated 1.7 million new infections in 2019 (UNAIDS 2019). The countries most affected are largely in sub-Saharan Africa, with South Africa reporting a prevalence of more than 13% of its population (StatsSA 2020). Only 70% of these individuals are currently undergoing therapy and of these individuals, approximately 64% have successful viral suppression (UNAIDS 2020). Challenges arise due to the cost of therapies as well drug-associated adverse effects, leading to drug non-compliance (Nagpal et al. 2010; Bor et al. 2013; Tadesse et al. 2014).

Current therapies largely focus on the three main enzymes of the viral life cycle, with the biggest targets being reverse transcriptase and protease. The general initial regimen consists of a nucleoside and non-nucleoside reverse transcriptase inhibitor along with a protease inhibitor (Riddler et al. 2008). If resistance occurs during these first-line therapies, an additional second or third-line therapy becomes an option that makes use of drugs that target integrase or viral entry (Bhatti et al. 2016). There are currently three entry inhibitors in clinical use. These are Enfuvirtide, Maraviroc and more recently, Ibalizumab. Enfuvirtide is a 36 amino acid polypeptide that is homologous to a section from gp41 (residues 643–678) and targets this viral protein (LaBonte et al. 2003). The binding of Enfuvirtide to gp41 prevents the required conformational changes from taking place and thus inhibits the fusion of the viral membrane with the host cell (Greenberg and Cammack 2004). The other two entry inhibitors target the host proteins, with Ibalizumab binding to the CD4 receptor. Ibalizumab is a monoclonal antibody fragment that binds to domain two of CD4 and prevents the viral V3 loop of gp120 from binding to the co-receptors (Burkly et al. 1992; Moore et al. 1992). The last of these inhibitors is Maraviroc, which is the only small molecule of these three, targeting the CCR5 co-receptor. Although effective, these drugs must still be used in combination with other HIV inhibitors as resistance is a

challenge when used as monotherapy (Wei et al. 2002; Pace et al. 2013; Lin et al. 2017). Maraviroc is the easiest to administer, with Enfuvirtide and Ibalizumab requiring invasive subcutaneous or intravenous administration (Zhang et al. 2002; Iacob and Iacob 2017). Enfuvirtide and Ibalizumab are associated with adverse effects, such as injection site reactions (Jamjian and McNicholl 2004; Beccari et al. 2019), while Maraviroc has been associated with more severe adverse effects which include liver toxicity and cardiac complications. Additionally, these drugs are extremely costly, where Ibalizumab has a cost of more than \$1000 for a single dose vial (Beccari et al. 2019). There is, therefore, a need for new drugs, which would be less toxic and more cost-effective. This study investigated metal-based complexes as potential new drugs against HIV entry.

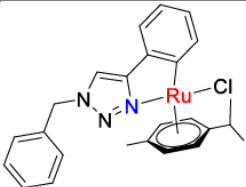
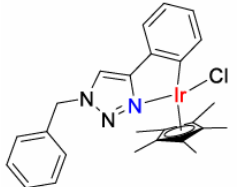

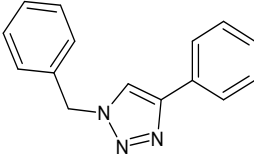
Metallo drugs have shown promising results in treating cancers, with the very well-known platinum-based drug Cisplatin and its derivatives being used in cancer therapy (Rosenberg et al. 1969). Several metal-based complexes are currently in clinical trials or have recently been approved, and examples include Nedaplatin, Heptaplatin, Lobalatin and TLD-1433 (Smithen et al. 2020; Yousuf et al. 2021). The addition of metals to organic compounds offers additional options in drug design, where the oxidation states of the metals, as well as the geometries of the metals to the bound ligand, could play a role in drug activity. This gives options outside of the usual geometries seen with organic molecules (tetrahedral, planar, trigonal-planar, or linear) and can give rise to new geometries which could include square-pyramidal- and octahedral geometries, due to the higher coordination numbers of the metals (Noffke et al. 2012). That being said, the ligand structure bound to the metal plays a particularly important role in the activity of the metal-based complexes, as alterations in the ligand structure can increase or decrease the activity of the metal-based complex (Leung et al. 2013).

Most of the research on the anti-HIV activity of metal-based complexes has mainly focussed on targeting reverse transcriptase and protease, with little focus on metal-based complexes targeting the entry aspect of the viral life cycle (Okada et al. 1993; Sechi et al. 2006; Sun et al. 2007; Fonteh and Meyer 2009; Gama et al. 2016). However, a study on dipicolylamine-zinc (II) complexes targeting CXCR4 has shown the potential for metal-based complexes to inhibit viral entry, and when Zinc (II) was

removed from these structures, the activity was reduced, demonstrating the importance of the zinc-(II) atom in binding to CXCR4 (Tamamura et al. 2006).

The metal-based complexes used in this study were previously analysed for potential anticancer abilities. These complexes were *N*-aryl-1H-1,2,3-triazole-based cyclometalated ruthenium-(II), osmium-(II), and iridium-(III) complexes (Table 1), with the geometries of the complexes being pseudo-octahedral. In the study done by Rono et al. (2019), these complexes showed promising results with modest- to good cytotoxic activities against lung-, cervical- and kidney cancer cells. The CC₅₀ values were determined (the concentration at which 50% of the cells are viable). The Iridium complex had the lowest CC₅₀ values, with the CC₅₀ values of the complexes obtained for lung cancer (4–20 μM), cervical cancer (29–70 μM), kidney cancer (9–80 μM) and leukaemia (25– > 100 μM) (Rono et al. 2019).

Table 1: The structures of the complexes investigated in the study

Name	Structure	Chemical formula	Molecular weight (g/mol)
<i>N</i>-aryl-1H-1,2,3-triazole-based cyclometalated ruthenium-(II) complex, Referred to as A		C ₂₅ H ₂₅ ClN ₃ Ru	504.010
<i>N</i>-aryl-1H-1,2,3-triazole-based cyclometalated iridium-(III) complex, Referred to as B		C ₂₅ H ₂₇ ClN ₃ Ir	597.173
<i>N</i>-aryl-1H-1,2,3-triazole-based cyclometalated osmium-(II) complex, Referred to as C		C ₂₅ H ₂₅ ClN ₃ Os	593.170
Ligand		C ₁₅ H ₁₃ N ₃	235.284

2 Materials and methods

The complexes (Table 1) used were obtained from C. Rono (University of Johannesburg's, Chemistry Department) where they were synthesised as previously described (Rono et al. 2019). The complexes were prepared for testing by dissolving them in DMSO and stored at $-20\text{ }^{\circ}\text{C}$. The final concentration of DMSO used during experimentation was below 0.2%.

2.1 Cell viability

The effects of the complexes on cell viability were analysed in Peripheral blood mononuclear cells (PBMCs) and TZM-bl cells which contain the necessary receptors for HIV infection. Ethics approval was obtained from the Faculty of Natural and Agricultural Sciences Ethics Committee (NAS041/2019) and HIV negative blood was drawn from consenting adults. The blood was diluted with RPMI 1640 media (1:1) and the diluted blood was layered onto Histopaque®-1077 in a 2:1 ratio and centrifuged (30 min, $1600\times g$). The layer of PBMCs was isolated following the gradient centrifugation. The isolated PBMCs were washed with RPMI 1640 media and centrifuged for 10 min at $860\times g$. To lyse any potential red blood cells, ammonium-chloride-potassium lysis buffer (ACK) (150 mM NH_4Cl , 10 mM KHCO_3 and 0.1 mM EDTA) was added and incubated with the cells for 5 min. The PBMCs were washed a second time with RPMI 1640 media at $258\times g$ for 10 min. Trypan blue-stained cells were counted using a Haemocytometer. Isolated cells were stimulated with $4\text{ }\mu\text{g/mL}$ phytohemagglutinin (PHA) for 2 h and added to 96 well plates (1×10^6 cells/mL per well). The cells were treated for 72 h with a serial dilution of the complexes and the anti-cancer drug Cisplatin (positive control that will indicate cytotoxicity), ranging from 100 to $1.56\text{ }\mu\text{M}$ in RPMI 1640 with 0.05% gentamicin and 1% antibiotic/antimycotic solution and 10% Fetal bovine serum (FBS). Following the treatment period, 3-(4,5-Dimethylthiazol-2-yl)-2,5-Diphenyltetrazolium Bromide (MTT) solution (5 mg/mL MTT in RPMI 1640 media, in a 1:5 ratio) was added and incubated overnight (Präbst et al. 2017). The formazan crystals that formed were solubilised using an acidic solution (1 M HCl and propanol in a 1:9 ratio). After a 15-min incubation period, the absorbance was measured at 550 nm and 690 nm using a SpectraMax® Paradigm® Multi-Mode Detection Platform plate reader (Molecular Devices, California, USA).

The effects of the complexes on cell viability were further analysed in TZM-bl cells which were grown in DMEM media containing 3.7 g/L of NaHCO_2 0.05% gentamicin,

1% antibiotic/antimycotic solution and 10% FBS. Once confluent, the cells were trypsinised and plated in a 96 well plate with 1×10^5 cells/mL per well. The cells were incubated overnight to allow for attachment and treated the following day with a serial dilution of the complexes and Cisplatin (positive control), ranging from 200 to 3.13 μ M. As was done with the PBMCs the cells were treated for 72 h following which the MTT assay was carried out as previously described and the absorbance measured.

2.2 Pseudo-virus production and treatment

The plasmids used for the production of the pseudo-viruses are available at the NIH AIDS reagent program and were obtained from the laboratory of Dr P Mthunzi-Kufa (CSIR, South Africa). The HIV-1 SG3 Δ Env Non-infectious Molecular Clone is originally from Drs. J. Kappes and X. Wu. The Env expressing plasmid, CAP210.2.00.E8, SVPC17 is originally from Drs. L. Morris, K. Mlisana and D. Montefiori. The Env expressing plasmid Du156, clone 12 (SVPC3) is originally from Drs. D. Montefiori, F. Gao, S. Abdool Karim, G. Ramjee. The Env expressing plasmid HIV-1 Env Expression Vector (Q23.ENV.17) is originally from Dr J. Overbaugh.

To produce pseudo-virus, a backbone expressing plasmid (HIV-1 SG3 Δ Env) and envelope expressing plasmid was propagated and used in combination. Three envelope expressing plasmids were used and propagated in *Escherichia coli* DH5 α , CAP 210 (subtype C), Du 156 (subtype C) and Q 23 (subtype A). The backbone expressing plasmid was propagated in *MAX Efficiency™ Stbl2™ Competent Cells* (Invitrogen, California, USA). HEK 293T-cells were required for transfection and were grown in DMEM as was done with the TZM-bl cells. Once confluent, 3×10^6 cells were seeded into a fresh flask and allowed to attach overnight. These cells were co-transfected with 5 μ g of Env expressing plasmid and 10 μ g of backbone expressing plasmid using the PolyFect transfection reagent (Qiagen, Hilden, Germany) with the adjustments in the protocol as described by (Montefiori 2004; Lugongolo et al. 2017). After 48 h of incubation, the pseudo-viruses were harvested using a 0.45 μ m filter. To determine the concentration of pseudo-virus isolated, a titre was performed following the methods described by (Montefiori 2004). TZM-bl cells which have been modified from HeLa cells to contain the necessary receptors for infection to take place, as well as a luciferase reporter gene that is upregulated following HIV infection, were used (Platt et al. 1998; Wei et al. 2002; Montefiori 2004). To examine the inhibition of the complexes, the pseudo-viruses (200 TCID₅₀) were pre-treated for an hour with the

complexes. Nevirapine was used as a positive control at 0.22 μM which has been shown to inhibit HIV pseudo-viruses previously (Prokofjeva et al. 2011). To all the wells 1×10^3 TZM-bl cells/mL were added with DEAE at a final concentration of 25 $\mu\text{g/mL}$ (Montefiori 2004). These plates were incubated for 48 h and following the incubation, media was removed until 50 μL remained. An equivalent amount of BrightGlo™ (Promega Corporation, Wisconsin, USA) containing luciferase substrate was added to all the wells and the solution was incubated for two minutes to lyse the cells. The supernatant was transferred to a black 96 well plate and the luminescence was measured using the SpectraMax® Paradigm® Multi-Mode Detection Platform plate reader.

2.3 *In silico* docking of the complexes

To identify a potential mechanism of action of the complexes *in silico* docking was carried out using Maestro 12.2 by Schrödinger (New York City, USA). The options available to dock metal-based complexes is very limited due to the available force fields which cannot model the interactions because of the metals (Hu and Shelver 2003; Adeniyi and Ajibade 2013). Docking metal-based complexes in Maestro is possible, however, does require alternative methods for preparing the ligands for docking (Adeniyi and Ajibade 2013). As the complexes contain metal ions, the structures had to be edited to create zero-order bonds to the metals before preparation could take place. The complexes, controls and proteins were prepared as described by Adeniyi and Ajibade (2013) using the protein preparation function since the usual ligand preparation method did not generate three-dimensional structures for the metal-containing ligands (Adeniyi and Ajibade 2013). Glide was used to define the docking site, based on the binding site of the ligand co-crystalised to the protein as obtained from the protein data bank (PDB). The proteins used for docking were those involved in the viral entry; CD4 (PDB code 2NY4), CCR5 (PDB code 4MBS), gp120 (PDB code 4RZ8) and gp41 (PDB code 2KP8). The prepared complexes were docked to the prepared proteins using the extra precision option with the OPLS3e force field and a GlideScore generated (Friesner et al. 2004).

Following the docking further *in silico* analyses were done to determine the potential uptake of the complexes. This was important to ensure the complexes will be bioavailable in the body. The Octanol–water partition coefficient (logP) value was determined. Potential cellular uptake was analysed by looking at the volume of the

complexes and the Molecular polar surface area. These analyses were done using Molinspiration Cheminformatics (Nová, Slovakia).

2.4 Statistical analysis

Each experiment was conducted in triplicate and three biological repeats were done. The CC_{50} values and statistical analyses were conducted using GraphPad Prism 9, version 9.3.1 (GraphPad Software, California, USA). One-way analysis of variance (ANOVA) followed by Dunnett's post hoc test was used to evaluate the statistical differences between the compound percentage viral inhibition and the untreated virus control. Differences were considered statistically significant from the controls when $P < 0.05$.

3 Results and discussion

3.1 Cytotoxic analysis of the complexes

The toxicities of the complexes in PBMCs and TZM-bl cells were evaluated to determine the non-toxic concentrations for use in downstream experimentation. The complexes were found to have lower CC_{50} values in PBMCs compared to TZM-bl cells (Table 2). The complexes **A** and **C** were non-toxic in TZM-bl cells, as none of the tested concentrations caused a decrease in viability values to below 50%, while complex **B** on the other hand, had the highest toxicity in both cell lines with the lowest CC_{50} values ($13.09 \pm 3.18 \mu\text{M}$ in PBMCs and $36.13 \pm 2.99 \mu\text{M}$ in TZM-bl cells) (Supporting information, Figs. S1, S2). This toxicity could be due to the characteristic reactivity of the iridium-(III) complex ion and the relatively high rate of hydrolysis (Rono et al. 2019). The ligand was analysed in TZM-bl cells for use in downstream experimentation, with pseudo-virus inhibition. The ligand was found to be non-toxic, as none of the tested concentrations resulted in percentage cell viability values below 50% (Supporting information, Fig. S1). With complex **B**, the aggregation of the complex was observed at higher concentrations, leading to reduced availability in the wells (Fig. S2).

The CC_{50} values of Cisplatin were not as low as expected, however, falling within a range (10–180 μM) of values previously reported for Cisplatin on various other cell lines (Islami-Moghaddam et al. 2009; Varela-Ramirez et al. 2011; Bennukul et al. 2014; Mora et al. 2019). The differences in cytotoxicity in these cell lines could be due

to varying degrees of resistance. This is due to Cisplatin not accumulating in resistant cells as it does in non-resistant cells (Shen et al. 2012).

Table 2: CC₅₀ values of the complexes in PBMCs and TZM-bl cells.

Complex	CC₅₀ ± SEM (µM) in PBMCs	CC₅₀ ± SEM (µM) in TZM-bl cells
A	24,36 ± 5,98	>200
B	13,09 ± 3,18	36,13 ± 2,99
C	29,16 ± 8,03	>200
Cisplatin	49,09 ± 3,26	43.52 ± 3,45

For downstream experimentation, the CC₅₀ values from PBMCs were used. There were a few reasons for this. Firstly, PBMCs give a much better representation of the toxicity in physiological conditions compared to TZM-bl cells. Secondly, PBMCs consist partly of CD4 cells which HIV naturally infects. Finally, downstream experimentation was carried out using TZM-bl cells, due to the luciferase reporter gene and the CC₅₀ values from the PBMCs were not toxic to TZM-bl cells.

3.2 In vitro inhibition of HIV pseudo-viruses

The pseudo-viruses were pre-treated with the complexes and allowed to infect TZM-bl cells (Figure 1). Infected cells produce luciferase based on the luciferase reporter gene (Montefiori, 2004, Wei *et al.*, 2002). Inhibition of the three metal-based complexes were found to be statistically significant compared to the untreated virus ($P < 0,05$), with the exception of treatment of Q 23 with **A** (P -value of 0.053). The ligand did not have a significant reduction in luciferase production in the pre-treated cells, with 13, 8% inhibition at 30 µM (Supporting information, Figure S3). This indicates the importance of the metals complexes in the inhibition of the pseudo-viruses. The complexes at the starting concentrations of the dilutions had comparable inhibition to the positive control Nevirapine (0, 22 µM), where the control exhibited between 68% and 86% inhibition of the different pseudo-viruses.

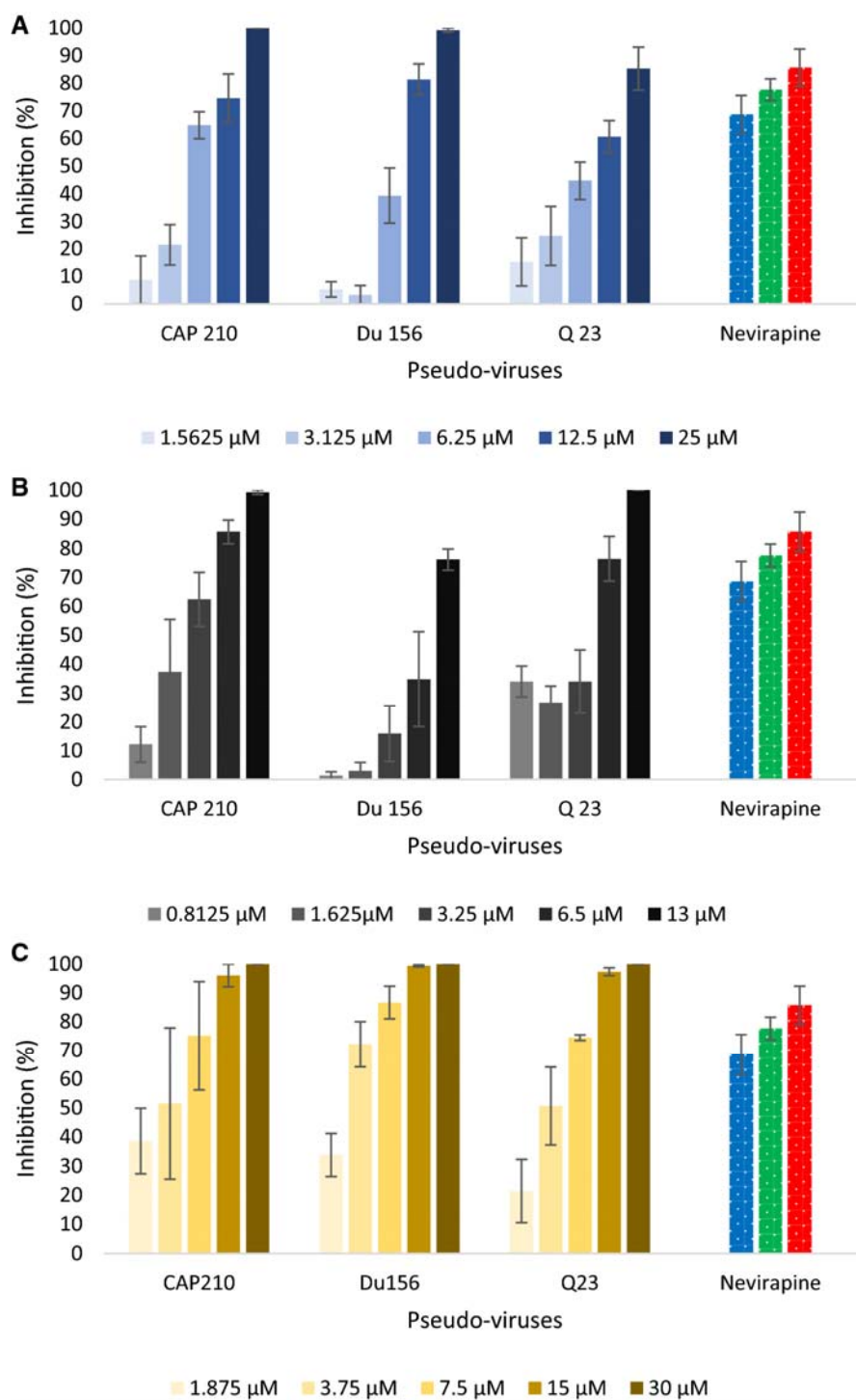


Figure 1: Percentage inhibition of the pseudo-viruses (CAP 210, Du 156 and Q 23) after treatment with the complexes. The control was Nevirapine at 0,22 μ M, with the inhibition in CAP 210 displayed in blue, Du 156 in green and Q 23 in red. **A.** The inhibition of the pseudo-viruses with *N*-aryl-1H-1,2,3- triazole-based cyclometalated ruthenium-(II) complex (**A**). **B.** The inhibition of the pseudo-viruses with *N*-aryl-1H-1,2,3- triazole-based cyclometalated iridium-(III) complex (**B**). **C.** The inhibition of the pseudo-viruses with *N*-aryl-1H-1,2,3- triazole-based cyclometalated osmium-(II) complex (**C**). The inhibition values are reported as mean \pm SEM for n=3. The graphs were normalised for values above 100% and below 0%.

To eliminate any false positives, the complexes were analysed for potential inhibition of the luciferase enzyme and none of the complexes exhibited enzyme inhibition (Supporting information, Fig. S4). The complexes exhibited inhibition of the pseudo-viruses at low micromolar IC₅₀ values (Table 3). These IC₅₀ values were used to determine the selectivity index (SI) of each complex by comparing the IC₅₀ values to the CC₅₀ values in TZM-bl cells (Table 4).

Table 3: The IC₅₀ values of the complexes in the pseudo-viruses.

Complexes	CAP 210	Du 156	Q 23
A (μM ± SEM)	5,34 ± 0,75	7,37 ± 0,73	7,41 ± 0,76
B (μM ± SEM)	2,35 ± 0,30	8,09 ± 1,68	3,18 ± 0,28
C (μM ± SEM)	4,18 ± 2,22	2,59 ± 0,35	3,73 ± 0,80

Table 4: The SI values of the complexes.

Complex/ Pseudo virus	SI value		
	CAP 210	Du 156	Q 23
A	>37.45	>27.14	>26.99
B	15.37	4.47	11.36
C	>47.85	>77.22	>53.62

The higher the SI value, the more effective the complex was and less toxic to uninfected cells at these effective concentrations. *N*-aryl-1H-1,2,3-triazole-based cyclometalated osmium-(II) complex (**C**) had the highest SI values, greater than 47,85, 77.22 and 53.62 for the three pseudo-viruses respectively. This indicated that the complexes were selective to the virus (Ashok et al. 2015). These SI values, however, were not as highly selective as many of the current HIV drugs, which are in the hundreds to thousands (Pauwels et al. 1993; Yuan et al. 2011; Cheng et al. 2016). The SI values of the complexes indicate there is great selectivity, however, structural improvements could result in improved selectivity.

3.3 In silico analysis of the complexes

Since the complexes had inhibitory effects on the pseudo-viruses, it was important to identify the potential mechanism of action. The potential mechanism of action was determined through the in silico docking (using Maestro 12.2) of the complexes with

four (CD4, CCR5, gp120 and gp41) of the main proteins involved in the viral entry. The complexes were docked and the obtained docking scores were compared to the docking scores of the co-crystallised ligands, which are known inhibitors (Table 5). The exception was with CD4, as the PDB structure did not have a ligand bound but had antibody fragments and gp120 bound. For this protein, docking was performed by creating a Glide grid around Phe 43 of CD4, since this amino acid has been shown to have many important interactions with gp120 (Kwong et al. 1998)

Table 5: Docking scores of the complexes against the proteins involved in viral entry into the host cell.

Complexes	Protein (PDB code)	Glide docking score
Maraviroc (Control)	CCR5 co-receptor (4MBS)	-10,342
A	CCR5 co-receptor (4MBS)	-9,294
C	CCR5 co-receptor (4MBS)	-6,455
Ligand	CCR5 co-receptor (4MBS)	-6,388
B	CCR5 co-receptor (4MBS)	-5,126
XIG (Control)	gp41 (2KP8)	-4,716
B	gp41 (2KP8)	-3,104
A	gp41 (2KP8)	-2,189
Ligand	gp41 (2KP8)	-1,514
C	gp41 (2KP8)	Did not dock
NBD-11021 (Control)	gp120 (4RZ8)	-7,552
A	gp120 (4RZ8)	-4,264
Ligand	gp120 (4RZ8)	-4,201
C	gp120 (4RZ8)	-3,650
B	gp120 (4RZ8)	-3,353
B	CD4 (2NY4)*	-2,169
A	CD4 (2NY4)*	-1,140
Ligand	CD4 (2NY4)*	-0,815
C	CD4 (2NY4)*	-0,729

* 2NY4 consisted of multiple chains, only chain B (T-cell surface glycoprotein CD4) was used during docking. This allowed for the exposure of Phe 43.

The more negative the docking score, the better the interactions were between the ligand and protein. Generally, a good docking score starts from - 8 (Schrödinger 2017). This study used the reference value of - 5 from Adeniyi and Ajibade (2013) to

determine the acceptability of the obtained docking scores for metal-based complexes (Adeniyi and Ajibade 2013). The lowest negative docking scores obtained were with the CCR5 co-receptor, and this was the only protein where the complexes had docking scores that were below - 5. This could indicate that inhibition of the pseudo-viruses observed in vitro is potentially due to the binding of the complexes to CCR5. Based on this observation, only interactions with the CCR5 co-receptor are further discussed. These interactions were compared to Maraviroc, a CCR5 antagonist currently in clinical use. Similar to Maraviroc, the complexes were bound to a hydrophobic pocket and sub-pockets surrounded by the transmembrane regions (Fig. 2A). In previous mutagenesis studies with Maraviroc, there were 11 amino acids identified as being crucial for inhibition (Garcia-Perez et al. 2011; Scholten et al. 2012). All these interactions were present during the docking of Maraviroc (Fig. 2B, key amino acids circled in blue), indicating the accuracy of the docking strategy. All the complexes interacted with these key amino acids to a different degree, with **A** interacting with nine, **B** with six and **C** with eight of the key amino acids (Fig. 2C–E, key amino acids circled in blue). Based on this finding, the more the complexes interacted with the key amino acids, the better the docking score was. Complexes **A** and **B**, formed pi-cationic interactions with Trp 86 of the co-receptor while Tyr 108 formed another pi-cationic interaction with ruthenium (**A**) (Fig. 2C, D). The geometries and oxidation states of the metal ions of the complexes could play a role in these interactions, where the complexes take up a pseudo-octahedral geometry (Leung et al. 2013; Rono et al. 2019). Predictably with the largely hydrophobic structures, there were many hydrophobic interactions, as seen with the green amino acids and the green lining surrounding the structures in Fig. 2B–E. Complex **A** and **C** had pi- stacking with the aromatic rings (residues 108–112), which was in the same region as with Maraviroc.

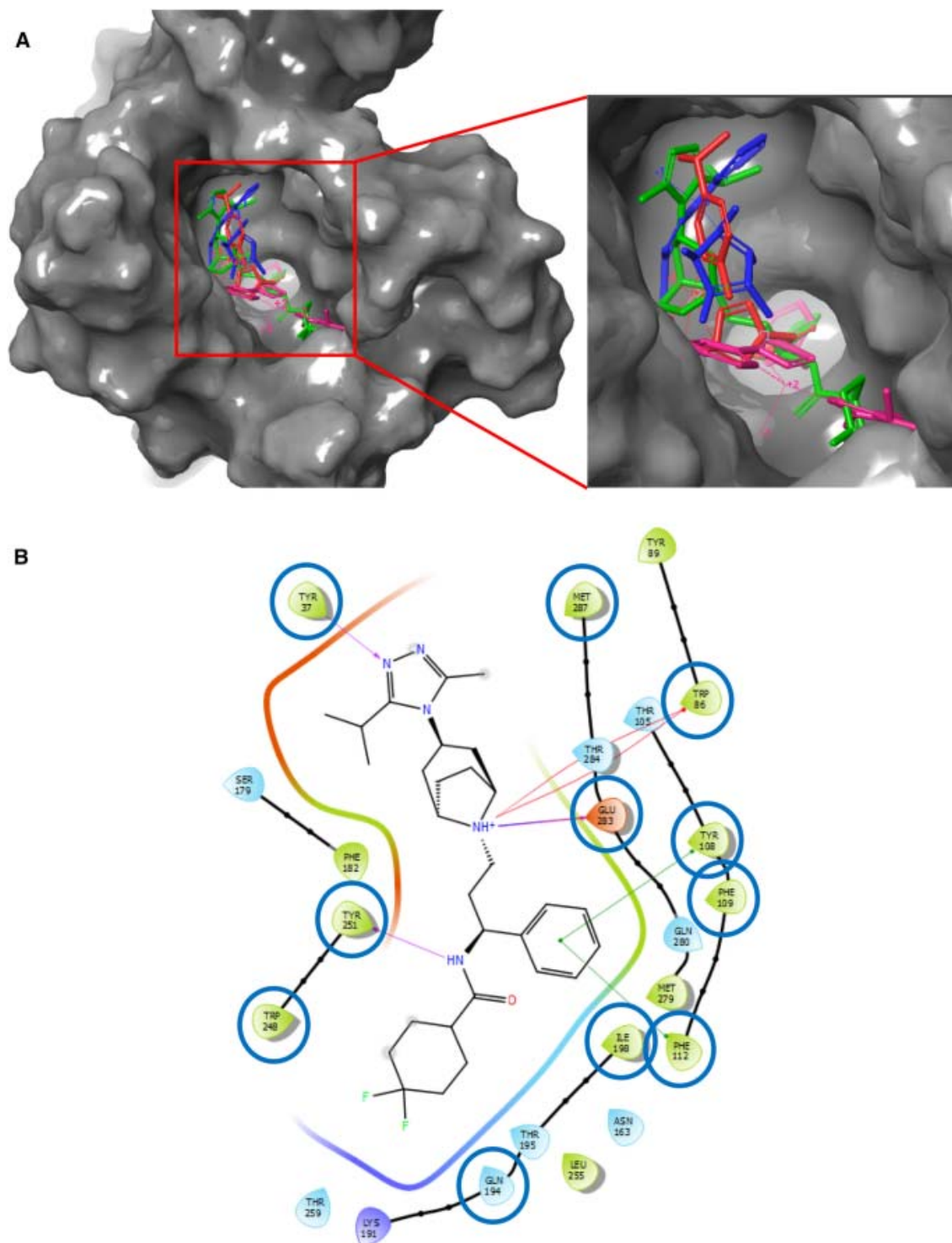


Figure 2: A. Docking images of the control Maraviroc and complexes. Ligand interactions of Maraviroc (green), *N*-aryl-1H-1,2,3- triazole-based cyclometalated ruthenium-(II) complex (**A**) (red), *N*-aryl-1H-1,2,3- triazole-based cyclometalated iridium-(III) complex (**B**) (blue) and *N*-aryl-1H-1,2,3- triazole-based cyclometalated osmium-(II) complex (**C**) (pink). **B-E.** Green lines show pi-pi stacking interaction in **B-E**, purple lines being hydrogen bonds, blue-red lines being salt bridge formations and red lines being pi-cationic interactions.

The complexes also interacted with key amino acids (Glu 283, Tyr 251 and Tyr 108) which play important roles in the binding of the V3 loop of gp120 to the CCR5 co-receptor. With these interactions being present, the binding of the complexes would prevent the Arg 18 of the V3 loop from interacting with the Glu 283, Tyr 251 and Tyr 108 of the co-receptor (Tamamis and Floudas 2014). These predicted interactions suggest that inhibition could potentially occur by preventing the viral gp120 from binding to CCR5.

To ensure the complexes can be bioavailable in the body, the cellular uptake of the complexes was predicted. Using Molinspiration Cheminformatics the LogP, volume and Molecular polar surface area were determined (Table 6).

Table 6: Cellular uptake prediction of the complexes

	A	B	C	Maraviroc
LogP	3.02	2.96	3.02	3.50
Molecular polar surface area (TPSA) (Å ²)	21.71	21.71	21.71	63.05
Volume	403.72	403.72	409.10	489.18

Comparing the complexes to Maraviroc in silico indicates that the complexes have potential bioavailability. Maraviroc has 23% absolute bioavailability (Abel et al. 2008). A negative LogP value indicates a higher concentration of the complex in the aqueous phase, whereas a positive value indicates a higher concentration in the lipid phase (Leo et al. 1971). The LogP value is lower than that of Maraviroc, with a lower value indicating potential better solubility in aqueous solutions compared to Maraviroc. Lower LogP values are usually found in drugs that are primarily found in aqueous regions like the blood, which is desired (Bhal 2007). The molecular polar surface area and volume indicate the potential uptake of the complexes from intestinal tissue (Ertl et al. 2000; Curreli et al. 2017). This indicates the bioavailability and transport of the complexes, with values below a TPSA of 140 Å² indicating good intestinal absorption (Anichina et al. 2021). These results indicate that the complexes do have the potential to be taken up through the intestinal wall and be bioavailable.

The future work includes chemical modification along with docking studies, with the desire to improve docking scores to the CCR5 co-receptor. Improved chemically

modified complexes could then be synthesised and analysed in vitro to improve the activity, with the desire of obtaining IC₅₀ values in the nanomolar range. Additionally, the complexes will be further analysed to confirm the mechanism of action in vitro using crystallisation techniques.

4 Conclusion

In conclusion, three complexes with good pseudo-virus inhibition at micromolar concentrations were analysed, and this inhibition was statistically significant ($P < 0.05$). In silico studies showed the presence of the metal ions in the ligand-co-receptor complex was essential for the observed inhibition. The potential mechanism of action of these complexes was through the interaction with the chemokine receptor, CCR5, resulting in the hindrance of gp120 binding. The data obtained support further investigation and chemical modification of these complexes to improve the activity.

5 Acknowledgements

We would like to thank the National Research Foundation of South Africa (NRF) and the University of Pretoria for funding the study. We would like to thank C. Rono for supplying the complexes used in the study.

6 Conflicts of interest

The authors declare no conflict of interest.

7 References

- Abel S, Russell D, Whitlock LA, Ridgway CE, Nedderman AN, Walker DK (2008) Assessment of the absorption, metabolism and absolute bioavailability of maraviroc in healthy male subjects. *Br J Clin Pharmacol* 65:60–67
- Adeniyi AA, Ajibade PA (2013) Comparing the suitability of autodock, gold and glide for the docking and predicting the possible targets of Ru (II)-based complexes as anticancer agents. *Molecules* 18:3760–3778
- Anichina K, Argirova M, Tzoneva R, Uzunova V, Mavrova A, Vuchev D, Popova-Daskalova G, Fratev F, Guncheva M, Yancheva D (2021) 1H-benzimidazole-2-yl hydrazones as tubulin-targeting agents: synthesis, structural characterization, anthelmintic activity and antiproliferative activity against MCF-7 breast carcinoma cells and molecular docking studies. *Chem Biol Interact* 345:109540
- Ashok P, Chander S, Balzarini J, Pannecouque C, Murugesan S (2015) Design, synthesis of new β -carboline derivatives and their selective anti-HIV-2 activity. *Bioorg Med Chem Lett* 25:1232–1235

- Beccari MV, Mogle BT, Sidman EF, Mastro KA, Asiago-reddy E, Kufel WD (2019) Ibalizumab, a novel monoclonal antibody for the management of multidrug-resistant HIV-1 infection. *Antimicrob Agents Chemother* 63:e00110-e119
- Bennukul K, Numkliang S, Leardkamolkarn V (2014) Melatonin attenuates cisplatin-induced HepG2 cell death via the regulation of mTOR and ERCC1 expressions. *World J Hepatol* 6:230
- Bhal SK (2007) LogP—Making sense of the value. *Advanced Chemistry Development*, Toronto, pp 1–4
- Bhatti AB, Usman M, Kandi V (2016) Current scenario of HIV/AIDS, treatment options, and major challenges with compliance to antiretroviral therapy. *Cureus* 8:e515
- Bor J, Herbst AJ, Newell M-L, Bärnighausen T (2013) Increases in adult life expectancy in rural South Africa: valuing the scale-up of HIV treatment. *Science* 339:961–965
- Burkly LC, Olson D, Shapiro R, Winkler G, Rosa J, Thomas D, Williams C, Chisholm P (1992) Inhibition of HIV infection by a novel CD4 domain 2-specific monoclonal antibody. Dissecting the basis for its inhibitory effect on HIV-induced cell fusion. *J Immunol* 149:1779–1787
- Cheng S, Wang Y, Zhang Z, Lv X, Gao GF, Shao Y, Ma L, Li X (2016) Enfuvirtide—PEG conjugate: a potent HIV fusion inhibitor with improved pharmacokinetic properties. *Eur J Med Chem* 121:232–237
- Curreli F, Kwon YD, Belov DS, Ramesh RR, Kurkin AV, Altieri A, Kwong PD, Debnath AK (2017) Synthesis, antiviral potency, in vitro ADMET, and X-ray structure of potent CD4 mimics as entry inhibitors that target the Phe43 cavity of HIV-1 gp120. *J Med Chem* 60:3124–3153
- Ertl P, Rohde B, Selzer P (2000) Fast calculation of molecular polar surface area as a sum of fragment-based contributions and its application to the prediction of drug transport properties. *J Med Chem* 43:3714–3717
- Fonteh P, Meyer D (2009) Novel gold (I) phosphine compounds inhibit HIV-1 enzymes. *Metallomics* 1:427–433
- Friesner RA, Banks JL, Murphy RB, Halgren TA, Klicic JJ, Mainz DT, Repasky MP, Knoll EH, Shelley M, Perry JK (2004) Glide: a new approach for rapid, accurate docking and scoring. 1. Method and assessment of docking accuracy. *J Med Chem* 47:1739–1749
- Gama NH, Elkhadir AY, Gordhan BG, Kana BD, Darkwa J, Meyer D (2016) Activity of phosphino palladium (II) and platinum (II) complexes against HIV-1 and *Mycobacterium tuberculosis* *Biometals* 29:637–650
- Garcia-Perez J, Rueda P, Alcamí J, Rognan D, Arenzana-Seisdedos F, Lagane B, Kellenberger E (2011) Allosteric model of maraviroc binding to CC chemokine receptor 5 (CCR5). *J Biol Chem* 286:33409–33421
- Greenberg ML, Cammack N (2004) Resistance to enfuvirtide, the first HIV fusion inhibitor. *J Antimicrob Chemother* 54:333–340

- Hu X, Shelver WH (2003) Docking studies of matrix metalloproteinase inhibitors: zinc parameter optimization to improve the binding free energy prediction. *J Mol Graph Model* 22:115–126
- Iacob SA, Iacob DG (2017) Ibalizumab targeting CD4 receptors, an emerging molecule in HIV therapy. *Front Microbiol* 8:2323
- Islami-Moghaddam M, Mansouri-Torshizi H, Divsalar A, Saboury A (2009) Synthesis, characterization, cytotoxic and DNA binding studies of diimine platinum (II) and palladium (II) complexes of short hydrocarbon chain ethyldithiocarbamate ligand. *J Iran Chem Soc* 6:552–569
- Jamjian MC, Mcnicholl IR (2004) Enfuvirtide: first fusion inhibitor for treatment of HIV infection. *Am J Health Syst Pharm* 61:1242–1247
- Kwong PD, Wyatt R, Robinson J, Sweet RW, Sodroski J, Hendrickson WA (1998) Structure of an HIV gp120 envelope glycoprotein in complex with the CD4 receptor and a neutralizing human antibody. *Nature* 393:648
- Labonte J, Lebbos J, Kirkpatrick P (2003) Enfuvirtide. Nature Publishing Group, Berlin
- Leo A, Hansch C, Elkins D (1971) Partition coefficients and their uses. *Chem Rev* 71:525–616
- Leung C-H, Zhong H-J, Chan DS-H, Ma D-L (2013) Bioactive iridium and rhodium complexes as therapeutic agents. *Coord Chem Rev* 257:1764–1776
- Lin H-H, Lee SS-J, Wang N-C, Lai Y, Kuo K, Weinheimer S, Lewis S (2017) Intramuscular Ibalizumab: pharmacokinetics, safety and efficacy vs IV Administration. In: Conference on Retroviruses and Opportunistic Infections
- Lugongolo MY, Manoto SL, Ombinda-Lemboumba S, Maaza M, Mthunzi-Kufa P (2017) The effects of low level laser therapy on both HIV-1 infected and uninfected TZM-bl cells. *J Biophotonics* 10:1335–1344
- Montefiori DC (2004) Evaluating neutralizing antibodies against HIV, SIV, and SHIV in luciferase reporter gene assays. *Curr Protoc Immunol* 64:12.11.1-12.11.17
- Moore J, Sattentau Q, Klasse P, Burkly L (1992) A monoclonal antibody to CD4 domain 2 blocks soluble CD4-induced conformational changes in the envelope glycoproteins of human immunodeficiency virus type 1 (HIV-1) and HIV-1 infection of CD4+ cells. *J Virol* 66:4784–4793
- Mora M, Gimeno MC, Visbal R (2019) Recent advances in gold–NHC complexes with biological properties. *Chem Soc Rev* 48:447–462
- Nagpal M, Tayal V, Kumar S, Gupta U (2010) Adverse drug reactions to antiretroviral therapy in AIDS patients at a tertiary care hospital in India: a prospective observational study. *Indian J Med Sci* 64:245
- Noffke AL, Habtemariam A, Pizarro AM, Sadler PJ (2012) Designing organometallic compounds for catalysis and therapy. *Chem Commun* 48:5219–5246

- Okada T, Patterson BK, Ye S-Q, Gurney ME (1993) Aurothiolates inhibit HIV-1 infectivity by gold (I) ligand exchange with a component of the virion surface. *Virology* 192:631–642
- Pace CS, Fordyce MW, Franco D, Kao C-Y, Seaman MS, Ho DD (2013) Anti-CD4 monoclonal antibody ibalizumab exhibits breadth and potency against HIV-1, with natural resistance mediated by the loss of a V5 glycan in envelope. *JAIDS J Acquir Immune Defic Syndr* 62:1–9
- Pauwels R, Andries K, Debyser Z, Van Daele P, Schols D, Stoffels P, De Vreese K, Woestenborghs R, Vandamme A-M, Janssen C (1993) Potent and highly selective human immunodeficiency virus type 1 (HIV-1) inhibition by a series of alpha-anilinophenylacetamide derivatives targeted at HIV-1 reverse transcriptase. *Proc Natl Acad Sci USA* 90:1711–1715
- Platt EJ, Wehrly K, Kuhmann SE, Chesebro B, Kabat D (1998) Effects of CCR5 and CD4 cell surface concentrations on infections by macrophagetropic isolates of human immunodeficiency virus type 1. *J Virol* 72:2855–2864
- Präbst K, Engelhardt H, Ringgeler S, Hübner H (2017) Basic colorimetric proliferation assays: MTT, WST, and resazurin. *Cell viability assays*. Springer, New York
- Prokofjeva M, Spirin P, Yanvarev D, Ivanov A, Novikov M, Stepanov O, Gottikh M, Kochetkov S, Fehse B, Stocking C (2011) screening of potential HIV-1 inhibitors/replication blockers using secure lentiviral in vitro system. *Acta Nat (англоязычная Версия)* 3:55
- Riddler SA, Haubrich R, Dirienzo AG, Peeples L, Powderly WG, Klingman KL, Garren KW, George T, Rooney JF, Brizz B (2008) Class-sparing regimens for initial treatment of HIV-1 infection. *N Engl J Med* 358:2095–2106
- Rono CK, Chu WK, Darkwa J, Meyer D, Makhubela BC (2019) Triazolyl Rull, RhIII, OsII, and IrIII complexes as potential anticancer agents: synthesis, structure elucidation, cytotoxicity, and DNA model interaction studies. *Organometallics* 38:3197–3211
- Rosenberg B, Vancamp L, Trosko JE, Mansour VH (1969) Platinum compounds: a new class of potent antitumour agents. *Nature* 222:385–386
- Scholten DJ, Canals M, Maussang D, Roumen L, Smit MJ, Wijtmans M, De Graaf C, Vischer HF, Leurs R (2012) Pharmacological modulation of chemokine receptor function. *Br J Pharmacol* 165:1617–1643
- Schrödinger (2017) 1: Maestro. Schrödinger LLC, New York
- Sechi M, Bacchi A, Carcelli M, Compari C, Duce E, Fisicaro E, Rogolino D, Gates P, Derudas M, Al-Mawsawi LQ (2006) From ligand to complexes: inhibition of human immunodeficiency virus type 1 integrase by β -diketo acid metal complexes. *J Med Chem* 49:4248–4260
- Shen D-W, Pouliot LM, Hall MD, Gottesman MM (2012) Cisplatin resistance: a cellular self-defense mechanism resulting from multiple epigenetic and genetic changes. *Pharmacol Rev* 64:706–721
- Smithen DA, Monro S, Pinto M, Roque J, Diaz-Rodriguez RM, Yin H, Cameron CG, Thompson A, McFarland SA (2020) Bis [pyrrolyl Ru (II)] triads: a new class of photosensitizers for metal–organic photodynamic therapy. *Chem Sci* 11:12047–12069

- Statssa SSA (2020) Statistical release: mid-year population estimates 2020. Africa SS, Pretoria
- Sun RW-Y, Ma D-L, Wong EL-M, Che C-M (2007) Some uses of transition metal complexes as anti-cancer and anti-HIV agents. *Dalton Trans* 2007:4884–4892
- Tadesse WT, Mekonnen AB, Tesfaye WH, Tadesse YT (2014) Self-reported adverse drug reactions and their influence on highly active antiretroviral therapy in HIV infected patients: a cross sectional study. *BMC Pharmacol Toxicol* 15:32
- Tamamis P, Floudas CA (2014) Molecular recognition of CCR5 by an HIV-1 gp120 V3 loop. *PLoS ONE* 9:e95767
- Tamamura H, Ojida A, Ogawa T, Tsutsumi H, Masuno H, Nakashima H, Yamamoto N, Hamachi I, Fujii N (2006) Identification of a new class of low molecular weight antagonists against the chemokine receptor CXCR4 having the dipicolylamine—zinc (II) complex structure. *J Med Chem* 49:3412–3415
- Tan Q, Zhu Y, Li J, Chen Z, Han GW, Kufareva I, Li T, Ma L, Fenalti G, Li J, Zhang W, Xie X, Yang H, Jiang H, Cherezov V, Liu H, Stevens RC, Zhao Q, Wu B (2013) Structure of the CCR5 chemokine receptor-HIV entry inhibitor maraviroc complex. *Science* 341(6152):1387–1390. <https://doi.org/10.1126/science.1241475>
- UNAIDS (2019) Global HIV & AIDS statistics—2019 fact sheet [Online]. UNAIDS. <https://www.unaids.org/en/resources/fact-sheet>. Accessed 11 May 2020
- UNAIDS (2020) UNAIDS Data 2020 [Online]. Geneva 2020: Joint United Nations Programme on HIV/AIDS. https://www.unaids.org/sites/default/files/media_asset/2020_aids-data-book_en.pdf. Accessed 7 Oct 2020
- Varela-Ramirez A, Costanzo M, Carrasco YP, Pannell KH, Aguilera RJ (2011) Cytotoxic effects of two organotin compounds and their mode of inflicting cell death on four mammalian cancer cells. *Cell Biol Toxicol* 27:159–168
- Wei X, Decker JM, Liu H, Zhang Z, Arani RB, Kilby JM, Saag MS, Wu X, Shaw GM, Kappes JC (2002) Emergence of resistant human immunodeficiency virus type 1 in patients receiving fusion inhibitor (T-20) monotherapy. *Antimicrob Agents Chemother* 46:1896–1905
- Yousuf I, Bashir M, Arjmand F, Tabassum S (2021) Advancement of metal compounds as therapeutic and diagnostic metallodrugs: current frontiers and future perspectives. *Coord Chem Rev* 445:214104
- Yuan Y, Maeda Y, Terasawa H, Monde K, Harada S, Yusa K (2011) A combination of polymorphic mutations in V3 loop of HIV-1 gp120 can confer noncompetitive resistance to maraviroc. *Virology* 413:293–299
- Zhang X, Nieforth K, Lang JM, Rouzier-Panis R, Reynes J, Dorr A, Kolis S, Stiles MR, Kinchelov T, Patel IH (2002) Pharmacokinetics of plasma enfuvirtide after subcutaneous administration to patients with human immunodeficiency virus: inverse Gaussian density absorption and 2-compartment disposition. *Clin Pharmacol Ther* 72:10–19